EXHIBIT 2

diffusivities between the SCF and the catalyst surface and of reduced coke deposition, benefits that have no parallel in homogeneous catalysis. The restriction to nonpolar or weakly polar reactants has been overcome through the use of entrainers or surfactants. For example, DeSimone and others have cleverly used soluble fluoropolymers in small amounts as surfactants to achieve greater rates or uniformity of product particle size during polymerization of methylmethacrylate (*47*) or acrylamide (*48*) in $scCO_2$. A similar approach could be used for molecularly catalyzed polar reactions in $scCO_2$.

The industrial outlook for SCFs as reaction media may be favorable because of the beneficial environmental effect of dispensing with organic liquid solvents. High-pressure operations would be facilitated in large-scale production processes and especially continuous-flow systems for which SCFs are well suited. Because of the nontoxicity of $scCO_2$, a future direction for molecular catalysis in that medium could be pharmaceutical synthesis. This is a field in which homogeneous transition metal-based catalysts have had a great impact. It is certain that researchers of homogeneous catalysis will adopt SCF as media for many more reactions and thus broaden the scope of this technique.

REFERENCES AND NOTES

1. R. Noyori, *Science* **248**, 1194 (1990).
2. ———, *Asymmetric Catalysis in Organic Synthesis* (Wiley, New York, 1994).
3. B. Subramaniam and M. A. McHugh, *Ind. Eng. Chem. Process Des. Dev.* **25**, 1 (1986).
4. J. F. Brennecke, *ACS Symp. Ser.* **514**, 201 (1993).
5. E. Kiran and J. M. H. Levelt Sengers, Eds., *Supercritical Fluids Fundamentals for Application*, vol. 273 of the NATO ASI Series E (Kluwer Academic, Dordrecht, Netherlands, 1994).
6. G. M. Kramer and F. Leder, U.S. Patent 3 880 945 (1975).
7. J. W. Rathke, R. J. Klingler, T. R. Krause, *Organometallics* **10**, 1350 (1991).
8. P. G. Jessop, T. Ikariya, R. Noyori, *Nature* **368**, 231 (1994).
9. K. P. Johnston and C. Haynes, *AIChE J.* **33**, 2017 (1987).
10. S. Kim and K. P. Johnston, *ACS Symp. Ser.* **329**, 42 (1987).
11. R. W. Shaw, T. B. Brill, A. A. Clifford, C. A. Eckert, E. U. Franck, *Chem. Eng. News* **69** (no. 51), 26 (1991).
12. G. J. Tawa and L. R. Pratt, *J. Am. Chem. Soc.* **117**, 1625 (1995).
13. K. D. Bartle, A. A. Clifford, S. A. Jafar, G. F. Shilstone, *J. Phys. Chem. Ref. Data* **20**, 713 (1991).
14. M. E. Sigman, S. M. Lindley, J. E. Leffler, *J. Am. Chem. Soc.* **107**, 1471 (1985).
15. Y. Ikushima, N. Saito, M. Arai, *J. Phys. Chem.* **96**, 2293 (1992).
16. J. A. Hyatt, *J. Org. Chem.* **49**, 5097 (1984).
17. C. Reichardt, *Chem. Rev.* **94**, 2319 (1994).
18. D. K. Dandge, J. P. Heller, K. V. Wilson, *Ind. Eng. Chem. Prod. Res. Dev.* **24**, 162 (1985).
19. P. G. Jessop, Y. Hsiao, T. Ikariya, R. Noyori, *J. Am. Chem. Soc.* **116**, 8851 (1994).
20. R. J. Klingler and J. W. Rathke, *ibid.*, p. 4772.
21. Their work has been reviewed: M. Poliakoff and S. Howdle, *Chem. Br.* **1995**, 118 (1995).
22. S. M. Howdle, M. A. Healy, M. Poliakoff, *J. Am. Chem. Soc.* **112**, 4804 (1990), and references therein.
23. J. A. Banister *et al.*, *J. Organomet. Chem.* **484**, 129 (1994).
24. J. A. Banister, S. M. Howdle, M. Poliakoff, *Chem. Commun.* **1993**, 1814 (1993).
25. M. Jobling *et al.*, *ibid.* **1990**, 1287 (1990).
26. M. Jobling *et al.*, *ibid.*, p. 1762.
27. M. J. Clarke *et al.*, *Inorg. Chem.* **32**, 5643 (1993).
28. P. G. Jessop, T. Ikariya, R. Noyori, *Organometallics* **14**, 1510 (1995).
29. J. M. DeSimone, Z. Guan, C. S. Elsbernd, *Science* **257**, 945 (1992).
30. Z. Guan, J. R. Combes, Y. Z. Menceloglu, J. M. DeSimone, *Macromolecules* **26**, 2663 (1993).
31. J. E. Cottle, U.S. Patent 3 294 772 (1966).
32. B. Folie and M. Radosz, in *Proceedings of the Third International Symposium on Supercritical Fluids* (Strasbourg, France, 17 to 19 October 1994), pp. 281–286.
33. M. T. Reetz *et al.*, *Chimia* **47**, 493 (1993).
34. Y. Inoue, Y. Itoh, H. Kazama, H. Hashimoto, *Bull. Chem. Soc. Jpn.* **53**, 3329 (1980).
35. T. Ikariya, P. G. Jessop, R. Noyori, Japanese Patent Appl. 274721 (1993).
36. P. G. Jessop, Y. Hsiao, T. Ikariya, R. Noyori, *Chem. Commun.* **1995**, 707 (1995).
37. J. Xiao, S. C. A. Nefkens, P. G. Jessop, T. Ikariya, R. Noyori, in preparation.
38. T. Ohta *et al.*, *J. Org. Chem.* **52**, 3174 (1987).
39. X. Zhang *et al.*, *Synlett* **1994**, 501 (1994).
40. J. W. Rathke, R. J. Klingler, T. R. Krause, *Organometallics* **11**, 585 (1992); J. W. Rathke and R. J. Klingler, U.S. Patent 5 198 589 (1993).
41. H. H. Yang and C. A. Eckert, *Ind. Eng. Chem. Res.* **27**, 2009 (1988).
42. K. S. Jerome and E. J. Parsons, *Organometallics* **12**, 2991 (1993).
43. O. Aaltonen and M. Rantakylä, *Chemtech* **21**, 240 (1991).
44. A. J. Russell *et al.*, *ibid.* **24**, 33 (1994).
45. M. Buback, *Angew. Chem. Int. Ed. Engl.* **30**, 641 (1991).
46. G. Kaupp, *ibid.* **33**, 1452 (1994).
47. J. M. DeSimone *et al.*, *Science* **265**, 356 (1994).
48. F. A. Adamsky and E. J. Beckman, *Macromolecules* **27**, 312 (1994).
49. R. C. Reid, J. M. Prausnitz, B. E. Poling, *The Properties of Gases and Liquids* (McGraw-Hill, New York, ed. 4, 1987).
50. S. Angus, B. Armstrong, K. M. de Reuck, Eds., *International Thermodynamic Tables of the Fluid State: Carbon Dioxide* (Pergamon, Oxford, 1976).

51. We gratefully acknowledge the assistance and advice of Y. Hsiao, J. Xiao, and K. Aoyagi of ERATO.

RESEARCH ARTICLE

Structures of Metal Sites of Oxidized Bovine Heart Cytochrome c Oxidase at 2.8 Å

Tomitake Tsukihara, Hiroshi Aoyama, Eiki Yamashita, Takashi Tomizaki, Hiroshi Yamaguchi, Kyoko Shinzawa-Itoh, Ryosuke Nakashima, Rieko Yaono, Shinya Yoshikawa*

The high resolution three-dimensional x-ray structure of the metal sites of bovine heart cytochrome c oxidase is reported. Cytochrome c oxidase is the largest membrane protein yet crystallized and analyzed at atomic resolution. Electron density distribution of the oxidized bovine cytochrome c oxidase at 2.8 Å resolution indicates a dinuclear copper center with an unexpected structure similar to a [2Fe-2S]–type iron-sulfur center. Previously predicted zinc and magnesium sites have been located, the former bound by a nuclear encoded subunit on the matrix side of the membrane, and the latter situated between heme a_3 and Cu_A, at the interface of subunits I and II. The O_2 binding site contains heme a_3 iron and copper atoms (Cu_B) with an interatomic distance of 4.5 Å; there is no detectable bridging ligand between iron and copper atoms in spite of a strong antiferromagnetic coupling between them. A hydrogen bond is present between a hydroxyl group of the hydroxyfarnesylethyl side chain of heme a_3 and an OH of a tyrosine. The tyrosine phenol plane is immediately adjacent and perpendicular to an imidazole group bonded to Cu_B, suggesting a possible role in intramolecular electron transfer or conformational control, the latter of which could induce the redox-coupled proton pumping. A phenyl group located halfway between a pyrrole plane of the heme a_3 and an imidazole plane liganded to the other heme (heme a) could also influence electron transfer or conformational control.

Bovine heart cytochrome c oxidase is a large multicomponent membrane protein complex with molecular size of 200 kilodaltons comprising 13 different polypeptide subunits. Located in the subunits are two heme A moieties, two redox active copper sites, one zinc, one magnesium, and possibly some phospholipids as the intrinsic constituents (*1*, *2*). This enzyme is one of the most intriguing biological macromolecules in the cell. As the terminal enzyme of biological oxidation, it reduces O_2 to H_2O at an active site with the four redox active transition metals coupling to a proton pumping pro-

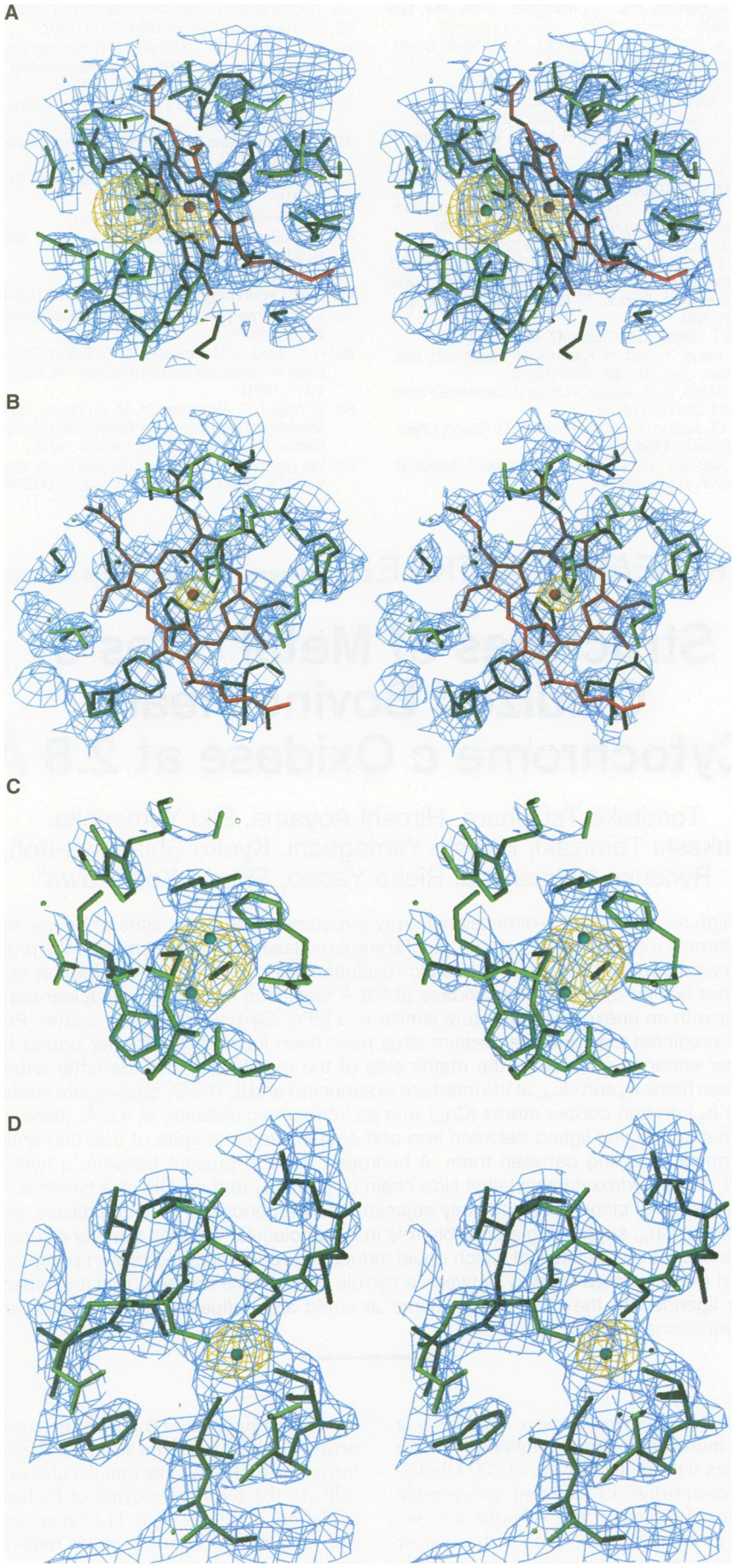

Fig. 1. Stereo pairs of the metal centers fitted in blue cages composed at 2σ of electron density at 2.8 Å resolution together with yellow or brown cages, drawn at 10 σ, of the native anomalous difference Fourier at 4.5 Å resolution. Model fitting was performed by the programs Turbo Frodo (*31*) and X-FIT in the program package QUANTA (CTC Laboratory Systems Co., Ltd.) on SGI workstations. (**A**) The oxygen binding and reduction site. The heme a_3 shown in red bars and a red ball, Cu_B in a green ball, and the amino acid residues in green bars are fitted well in the cages. (**B**) The heme a, two histidine ligands of Fe_a, and some amino acid residues are shown in the same colors as in (A). (**C**) Dinuclear structure of the Cu_A. Two copper atoms are shown with brown balls, amino acid residues with green bars, and tetrahedral coordination of each copper atom in blue dotted lines. (**D**) Tetrahedral coordination structure of the zinc site. Four cysteines and zinc atom position are shown with green bars and a dark yellow ball, respectively.

cess across the mitochondrial inner membrane (*2*, *3*). The bright green color of the enzyme, which is due to the heme iron and which changes sensitively with the redox and ligand-binding states of the active center, has stimulated electronic, resonance Raman, and infrared spectroscopic studies on its kinetic behavior during the enzymatic turnover (*2*–*4*).

Electron spin resonance studies have been made on the paramagnetic iron and copper ions (*2*, *3*), and infrared spectroscopy has been used to study various respiratory inhibitors as probes for the O_2 binding site (*5*). In addition, the varied roles of the large and complex protein moiety, which in the mammalian enzyme contains 13 different polypeptide subunits with 3 being coded by a mitochondrial and nuclear genes and 10 by a nuclear gene, have been widely studied (*1*, *6*). Thus, among the enzymes participating in biological oxidation, this one has been of primary interest ever since it was discovered (*7*). Despite these extensive and successful efforts, the absence of a crystal structure and analysis at atomic resolution has set limits on our understanding of the reaction mechanism of this enzyme. We had previously crystallized the enzyme from bovine heart, thus providing an example of x-ray diffractable crystals of a membrane protein isolated from a higher animal. However, the resolution of the crystals was far lower than suitable for x-ray structural analysis at atomic resolution (*8*). We therefore changed our techniques and have now ob-

T. Tsukihara, H. Aoyama, E. Yamashita, T. Tomizaki, and H. Yamaguchi are at the Institute for Protein Research, Osaka University, 3-2 Yamada-oka, Suita 565, Japan. K. Shinzawa-Itoh, R. Nakashima, R. Yaono, and S. Yoshikawa are at the Department of Life Science, Himeji Institute of Technology, Kamigohri Akoh, Hyogo 678-12, Japan.

*To whom correspondence should be addressed.

Table 1. Peak heights in the native electron density map at 2.8 Å and those in the anomalous difference Fourier map at 4.5 Å resolution.

Atomic group	Peak heights in σ unit	
	Electron density map	Anomalous difference map
Cu_A	12.1	14.3
Zn	10.9	9.7
Cu_B	11.4	9.3
Fe_{a_3}	10.3	5.1
Fe_a	10.0	5.3
PO^{4*}	9.6	
PO^{4*}	9.3	
PO^{4*}	8.3	
Other highest	7.8	3.5

*PO^4 represents a phosphate group of phospholipid.

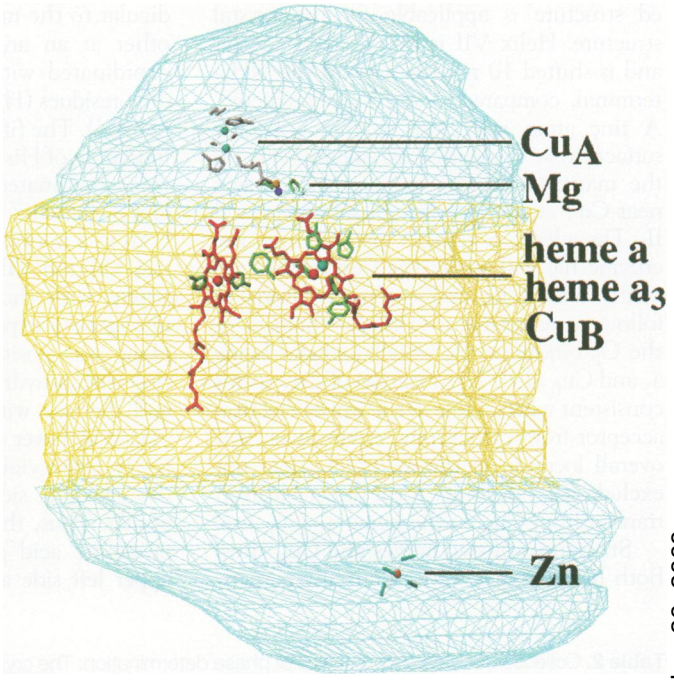

Fig. 2. A schematic representation of metal site location in beef heart cytochrome c oxidase. Molecular surface defined with the electron density map at 5 Å resolution is shown by the cage. The yellow, the upper light blue, and the lower light blue represent a transmembrane part with 48 Å thickness, a hydrophilic part protruding to the cytosolic side with 37 Å, and the other hydrophilic part with 32 Å in the matrix space, respectively. The three metal centers, Fe_a, Fe_{a_3} and Cu_B are located at the same level, 13 Å below the membrane surface on the cytosolic side. Another metal center, Cu_A, close to the molecular surface is 8 Å above the membrane surface level, and magnesium ion is at the membrane surface level. The distances of Cu_A-Fe_a, Cu_A-Fe_{a_3}, Cu_A-Mg, Fe_{a_3}-Fe_a, and Fe_{a_3}-Mg are 19 Å, 22 Å, 9 Å, 14 Å, and 15 Å, respectively.

tained crystals that diffract up to 2.6 Å resolution. During these procedures, it was necessary to adjust the structure of detergent that we used to stabilize the enzyme molecule in aqueous solution (9). We have now obtained from the electron density at 2.8 Å resolution the structures of the metal centers, which provide electron transfer pathways and serve as key structures for proton pumping.

Crystallization and structural determination. The crystals used for our study were prepared from bovine heart cytochrome c oxidase at the fully (resting) oxidized state (9) by the method previously described (*8*, *10*). Briefly, the purified protein was stabilized in aqueous solution with the nonionic detergent, 0.2 percent decyl maltoside in 40 mM sodium phosphate buffer, pH 6.8, and crystallized by the batch method from a solution where the protein concentration was 9.0 percent (w/v) at 4°C, and with polyethylene glycol 4000 (Sigma) being used as the precipitant. The crystals diffracted x-rays up to 2.6 Å resolution. This enzyme preparation reacted with cyanide monophasically, but not so rapidly as the enzyme under turnover conditions, indicating that it is the "fast" form (*11*).

We have obtained electron density of the enzyme at 2.8 Å resolution by the multiple isomorphous replacement (MIR) method; we then used a density modification procedure coupled with noncrystallographic symmetry (NCS) averaging. The electron density distribution obtained was so clear that all the metal center structures were easily built into the map (Fig. 1). The model building was performed with a modeling option REFINE of Turbo Frodo to fit each residue with standard dimensions in appropriate electron density cages. The final refinement comparing the obtained model and x-ray diffraction data has not yet been completed. However, the electron density distribution with extremely high reliability, evidenced by R_{free} factor of 0.258 at 2.8 Å resolution, allows quite satisfactory fitting of the atomic model to the electron density in most parts of the enzyme molecule, including the metal sites. It is remarkable that such a high accuracy of the electron density distribution has been obtained from such a large and multicomponent protein complex. The quality of the atomic model assignments is clearly shown by stereoscopic drawings of the model structures superimposed on electron density cages (Fig. 1).

The following results also indicate that the electron density distribution is plausible and thus reliable.

1) The order in peak height of the electron density map is consistent with the order in number of electrons of a group located at the corresponding peak (Table 1).

2) The anomalous difference Fourier map clearly revealed metal centers in spite of very low anomalous contribution from the metals compared with the structure factor of a whole molecule (Fig. 1 and Table 1). This is strong evidence of extremely high accuracy of phases and electron density.

3) Of 1850 amino acid residues, main chains of 1808 residues were successfully located in the map. More than 90 percent of side chains of nonglycine residues have reasonable electron density cages.

We now present the metal site structures of the enzyme at the fully (resting) oxidized state. Intensity data collection and phase determination are summarized in Table 2.

Overall location of metal sites. The membrane-embedded region evaluated from the start and end of the helices was 48 Å wide in the middle part of the molecule (Fig. 2). The direction of the molecules with respect to the cytosolic and matrix sides was estimated from the location of a copper site, Cu_A (see below), and the positions of the NH_2- and COOH-termini of peptide subunits. All the 13 subunits, each different from the other, were assigned in the crystal structure, which provides conclusive evidence that all these subunits are intrinsic constituents of the enzyme and that each is present in equimolar amount. This enzyme is in a dimeric state in the crystal, and there is no indication for strong interaction between the metal sites of each monomer. One of the redox active copper sites, Cu_A, was located in the third largest subunit, subunit II (6), which protrudes to the cytosolic side 8 Å above the membrane surface. The position of Cu_A, which is a dinuclear copper center (see below), is defined as the middle point between the two copper atoms. The other redox active metal centers, heme a, heme a_3, and Cu_B, the latter two of which constitute the O_2 binding and reduction site (*2*, *3*), were bound to subunit I at an identical level approximately 13 Å below (or inside) the membrane surface at the cytosolic side. Twelve transmembrane helices were found in subunit I, as has been predicted from the amino acid sequence (*1*, *12*). Although most of the helices in the crystal structure are longer than those predicted, the numbering of the helices for the predict-